VIII International Conference on Fracture Mechanics of Concrete and Concrete Structures
FraMCoS-8
J.G.M. Van Mier, G. Ruiz, C. Andrade, R.C. Yu and X.X. Zhang (Eds)

# TAILORING HIGH-STRENGTH SHCC

**A. P. FANTILLI[*], S. KWON[†], H MIHASHI[†] and T. NISHIWAKI[†]**

[*] Politecnico di Torino
Corso Duca degli Abruzzi 24, 10129 Torino, Italy
e-mail: alessandro.fantilli@polito.it , www.polito.it

[†] Tohoku University
Aramaki Aoba 6-6-11-1205, Aoba-ku, 980-8579 Sendai, Japan
e-mail: ty@archi.tohoku.ac.jp , www.archi.tohoku.ac.jp

**Key words:** High-Strength Concrete – HSC; Strain Hardening Cementitious Concrete – SHCC; Tensile tests; Fiber Volume Fraction; Crack Spacing.

**Abstract:** Multiple cracking and strain hardening can be achieved in cement-based specimens subjected to uniaxial tension by increasing the volume fraction of steel fibers with hooked ends, or by using plastic fibers with and without steel fibers, or by means of high bond steel fibers (e.g., twisted fibers or cords). To better understand why relevant mechanical performances are obtained in such situations, an analytical micro-mechanical model was proposed. The model, capable of predicting the average distance between cracks as measured in some experimental campaigns, is here used to tailor a high performance fiber-reinforced concrete. Specifically, a two High-Strength and Strain Hardening Cementitious Concrete (HS-SHCC), reinforced with different types of steel fibers, are introduced. By combining direct uniaxial tensile tests, performed on the so-called dumbbell-shaped specimens, and the results of the micro-mechanical model, the critical value of the fiber volume fraction can be evaluated. It should be considered as the minimum amount of long steel fibers which can lead to the formation of multiple cracking and strain hardening under tensile actions. The aim of the present paper is to reduce such volume as much as possible, in order to improve the workability and reduce the final cost of HS-SHCC.

## 1 INTRODUCTION

To tailor a High Strength Concrete (HSC), some special techniques and raw materials must be adopted (i.e., low water/cement ratio, presence of mineral admixtures, high strength coarse aggregate, etc.) [1]. As HSC generally fails in a brittle manner, in such concretes the presence of fibers is also necessary. However, the cost of large fiber volume content can be higher than that of cementitious matrix. Thus, the required ductility of HSC should be obtained by minimising, or optimizing, the amount of fiber [2].

According to Banthia and Sappakittipakorn [3], in hybrid Fiber Reinforced Concrete (FRC) <<*…there is positive interaction between the fibers and the resulting hybrid performance exceeds the sum of individual fiber performances. This phenomenon is often termed “Synergy”*>>. Combining fibers of different geometry is a possible manner to create this synergy. Indeed, short fibers enhance the fracture toughness of cementitious matrix in tension. Thus, after the initial elastic behaviour, the mechanical response of FRC can show a delayed micro-cracking stage (i.e., the second stage), because of the bridging action performed by the short thin fibers [4]. Conversely, the beneficial effects of long fibers are particularly evident in the third stage, and consist of arresting and delaying the growth of macro-cracks [5]. If the amount of long and short fibers is appropriately evaluated, it is possible to obtain a strain-hardening cementitious composite (SHCC), capable of developing more than one crack before the localization of tensile strains [6].

In what follows, two classes of High-Strength and Strain-Hardening Cementitious Composites (HS-SHCC) are investigated. Both the HS-SHCCs are reinforced with different amounts of long steel fibers, but only one of them also contains a fixed volume of short fibers. By means of experimental and theoretical analyses, the critical fiber volume fraction is herein evaluated. It should be considered as the minimum amount of long fibers which can lead to the formation of multiple cracking and strain hardening under tensile actions. The aim of the present paper is to reduce such volume as much as possible, in order to reduce the cost and improve the workability in both the HS-SHCCs.

## 2 CRACK SPACING AND FIBER VOLUME FRACTION OF SHCC

SHCC and reinforced concrete (RC) elements in tension can show similar response not only in terms of normal force $N$ – average strain $\varepsilon_m$, but also in terms of crack spacing (Fig.1). At the onset of cracking (around point A in Fig.1), $N$ is generally lower than cracking load $N_{cr}$, and the $N$-$\varepsilon_m$ diagram shows a softening branch. If these conditions persist for higher elongations, the failure of the structural elements occurs in the presence of a single crack. As depicted in Fig.1, this behaviour takes place not only in under-reinforced RC structures subjected to tensile loads, but also in FRC members with a low fiber volume fraction $V_f$.

At the point B of Fig.1, where $N = N_{cr}$, new cracks appear and, with the increase of elongation, strain hardening characterizes the $N$-$\varepsilon_{sm}$ diagram of normally reinforced RC and SHCC ties.

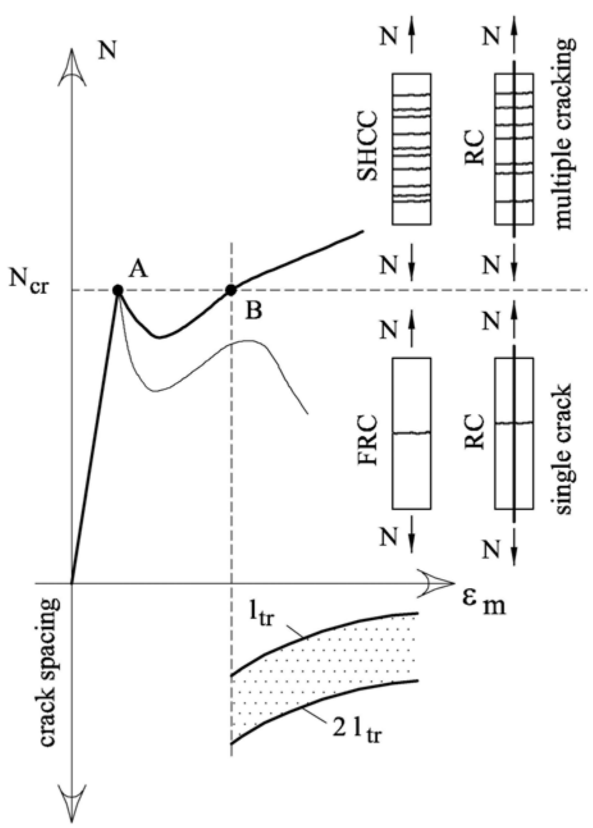


**Figure 1**: Mechanical behaviour of RC, FRC, and SHCC under tensile actions [7].

If the transmission length ($l_{tr}$) is assumed to be the length of the zone where slips occur between reinforcement and cementitious matrix [7], during the hardening stage the average crack spacing ranges between $l_{tr}$ and 2 $l_{tr}$ (Fig.1). Thus, the definition of $l_{tr}$ at the cracking load (i.e., point B of Fig.1) is of primary importance in evaluating the presence of multiple cracking and strain hardening response in SHCC composites.

The following value of the transmission length is obtained by adapting the tension-stiffening equations of RC structures to the fiber-matrix interaction (see Fantilli et al. [7]):

$$l_{tr} = -\frac{\ln\left[\dfrac{\left(p_f\ k_B\ V_f - 2A_f\, k_C\sqrt{\alpha}\right)}{\left(p_f\ k_B\ V_f + 2A_f\, k_C\sqrt{\alpha}\right)}\right]}{\sqrt{\alpha}} \tag{1}$$

where,

$$\alpha = \frac{p_f\, k_B}{A_f}\left(\frac{1}{E_f} + \frac{V_f}{E_c}\right) \tag{2}$$

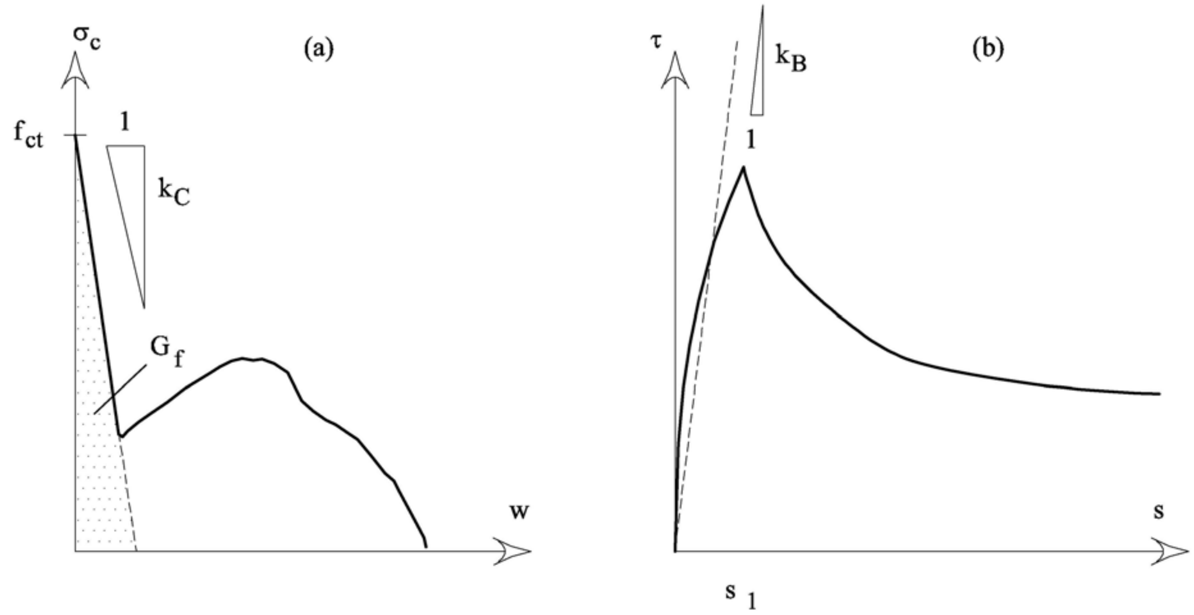


**Figure 2**: The cohesive and bond parameters: (a) fictitious crack model of cementitious matrix; (b) bond-slip relationship of fibers in cementitious matrix.

In both the equations, $A_f$ and $p_f$ are the area and perimeter of fiber cross-section, respectively; $E_c$ and $E_f$ are the Young's moduli of cement-based matrix and fiber, respectively; $k_C$ is the cohesive parameter; and $k_B$ is the bond parameter.

Since Eq.(1) is obtained in the situation when the first crack is growing (i.e., the crack width $w$ is nearly zero) and other cracks are going to develop (point B in Fig.1), $k_C$ is used to approximate the fictitious crack model $\sigma_c$-$w$ of the cementitious matrix. According to Fig.2a, this coefficient can be associated to the so-called Fracture Energy $G_f$, which differs from the work of fracture $G_F$ [8].

Similarly, the tension stiffening equations are here applied when slips are nearly zero, thus bond stresses are assumed to be in linear proportion (through the coefficient $k_B$ - Fig.2b) with slips. In other words, the bond-slip $\tau$-$s$ relationship is approximated by a linear secant model, in which also other phenomena, such as the snubbing of fiber pullout, are taken into consideration [7].

For a given SHCC, Eq.(1) provides the range of the possible crack spacing, which in turn depends on the amount of fiber-reinforcement (i.e., $V_f$).

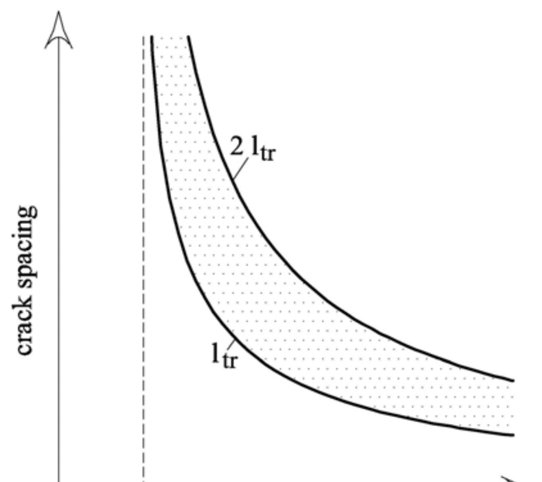


**Figure 3**: – Range of possible crack spacing values in SHCC [7].

Fig.3 shows the range, in terms of crack spacing vs. fiber volume fraction, as defined by Fantilli et al. [7]. If $V_f$ decreases, transmission length (and crack spacing) increases, and tends towards infinity when the fiber volume fraction reaches the following critical value [7]:

$$V_{f,cr} = \frac{A_f \; 2\left(k_C\right)^2}{E_c \; p_f \; k_B}\left(1+\sqrt{1+\frac{\left(E_c\right)^2 \; p_f \; k_B}{A_f \; E_s\left(k_C\right)^2}}\right) \tag{3}$$

Thus, the condition of multiple cracking and strain hardening cannot occur when $V_f \leq V_{f,cr}$ .

## 3 EXPERIMENTAL STUDY

In order to verify the applicability of the Eqs.(1)-(3) to HS-SHCC, an experimental campaign has been performed on two series of composites subjected to uniaxial tension. In the specimens of Series 1, different amounts of long steel fibers (having hooked ends) are added to a high-strength cementitious matrix, whose constituents are reported in Table 1.

**Table 1**: Constituent of the cementitious matrix.

| Material | Density (g/cm$^3$) | Properties |
|---|---|---|
| Binder | 3.01 | low heat cement (82%) and silica fume (18%) |
| Sand | 2.60 | Average diameter 0.212 mm |
| Wollastonite | 2.90 | |
| Superplasticizer | 1.05 | Polycarboxylic acid system |
| Antifoaming agent | 1.0 | |

**Table 2**: Properties of the steel fibers.

| Type | Density (g/cm$^3$) | Length (mm) | Diam. (μm) | Tensile strength (MPa) |
|---|---|---|---|---|
| OL | 7.85 | 6 | 160 | 2000 |
| HDR | 7.85 | 30 | 280 | 3000 |

Conversely, Series 2 consists of the same types of matrix and long fibers (in different contents), but also of short steel fibers (1% in volume). The main geometrical and mechanical properties of the long and short fibers, called respectively HDR and OL, are summarized in Table 2.

In the hybrid specimens of Series 2, the fiber volume fraction $V_f$ is only referred to the amount of HDR, whereas short OL fibers are assumed to be a part of the cement-based matrix. Indeed, according to Betterman et al. [5], hybrid composites show a multiscale structure of cracking, in which short fibers bridge microcracks, and long fibers prevent the sudden propagation of macro-cracks. Thus, short fibers (used to reinforce Series 2 specimens) can be assumed to be a part of the cement-based matrix. Under these conditions, Eqs.(1)-(3) can be applied to hybrid composites, if the coefficient $k_C$ (Fig.2a) is measured on specimen only reinforced by short fibers, and the fiber volume fraction $V_f$ is only referred to the amount of long fibers (i.e., HDR). However, in both the series, Young's modulus $E_c = 21$ GPa, cohesive parameter $k_C = 260$ MPa/mm, and tensile strength $f_{ct} = 14$ MPa define the uncracked and cracked stages of the high strength cementitious matrix with and without short fibers.

Both the series are composed by 4 groups, in the amount of long fibers varies from 0.5 to 2% in volume (see Table 3). Each group comprises five "dumbbell type" specimens. The geometrical dimensions of these specimens, tested in uniaxial tension and depicted in Fig.4a, are in accordance with the Recommendations of the Japan Society of Civil Engineers [9] for SHCC composites. Loads were vertically applied with a 30 kN capacity Instron testing machine, using "fix-fix" support conditions. Tests were controlled by vertical displacement at a velocity of 0.5 mm/min.

**Table 3**: The specimens tested in the present project.

| | | Fiber content | |
|---|---|---|---|
| Series | Group | OL (%) | HDR (%) |
| 1 | S1_05 | 0 | 0.5 |
| | S1_10 | 0 | 1.0 |
| | S1_15 | 0 | 1.5 |
| | S1_20 | 0 | 2 |
| 2 | S2_05 | 1.0 | 0.5 |
| | S2_10 | 1.0 | 1.0 |
| | S2_15 | 1.0 | 1.5 |
| | S2_20 | 1.0 | 2 |

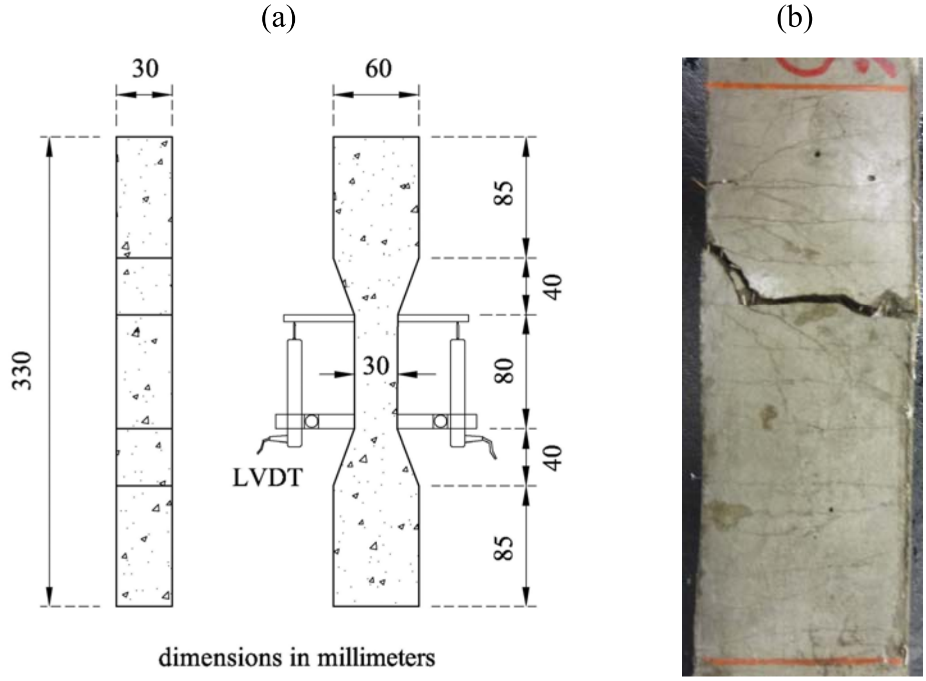


**Figure 4**: Uniaxial tensile tests: (a) geometrical properties of the “dumbbell type” specimens [9]; (b) multiple cracking in the central gauge length.

Average extension was measured over the central gauge length (80 mm) by means of two LVDTs, placed on the opposite side of the member and attached to mounting frames, firmly clamped on to the specimens. In this zone, before strain localization (Fig.4b), average crack spacing was also measured and compared with the theoretical prediction of the cohesive interface model introduced by Fantilli et al. [7].

## 4 EXPERIMENTAL RESULTS AND DISCUSSION

### 4.1 The stress-strain curves

Subjected to tensile actions, the specimens of Series 1 show the stress-strain curves depicted in Fig.5a-d. In the specimens S1_05 (Fig.5a) and S1_10 (Fig.5b), strain softening appears in the post cracking stage, and failure occurs in presence of a single crack. In accordance with Fig.1, such cement-based composites cannot be considered as SHCC.

The stress-strain curves of the hybrid composites are reported in Fig.5e-h.

Strain hardening is evident in all the specimens, except for those reinforced with 0.5% HDR (S2_05 - Fig.5e).

In the case of Series 1, only when the volume fraction of HDR is higher than 2%, the specimens show a maximum tensile stress higher than the strength of the cementitious matrix (about 5 %). Conversely, the specimens of Series 2 show a tensile strength higher than that of plain matrix even in the case of 1.5% in volume of HDR (about 14 % for S2_15 and 40 % for S2_20).

### 4.2 Crack spacing

When multiple cracking occurs, it is possible to measure the crack spacing, here considered as the ratio between the central gauge length of the specimen (i.e., 80 mm - Fig.4b), and the number of cracks. The values of the measured crack spacing are reported in Table 4. In all the cases, the higher the amount of HDR, the higher the number of cracks and the lower the crack spacing (see Table 4).

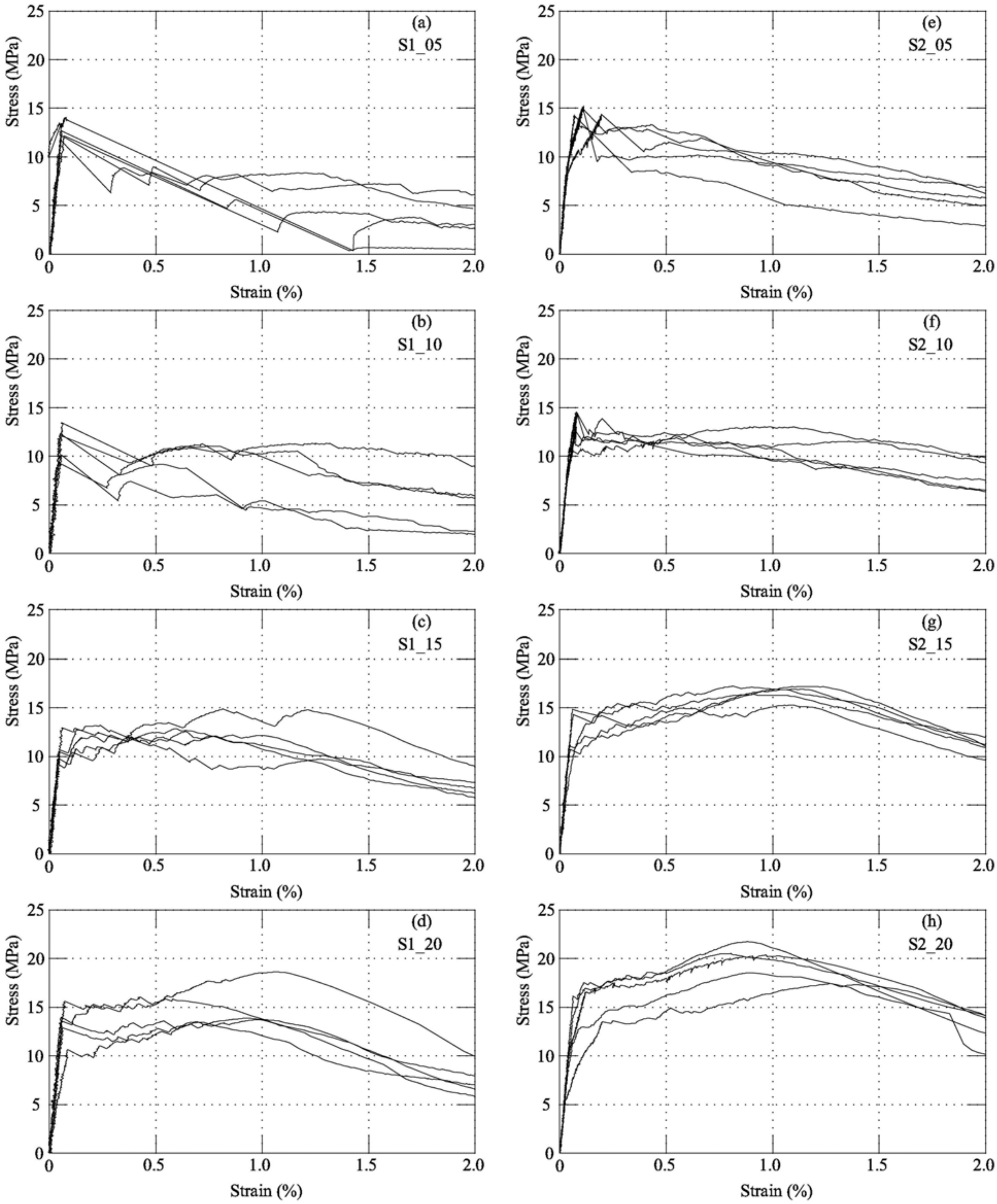


**Figure 5**: The stress-strain diagrams of the high strength concretes: (a)-(d) Series 1; (e)-(h) Series 2.

As mentioned before, only two type of specimens of Series 1 can show multiple cracking (i.e., S1_15 and S1_20), whereas in the case of hybrid composites, strain hardening can appear also in the presence of a lower volume of HDR ( ≥ 1 %).

**Table 4**: Crack spacing in the specimens tested in the present project.

| Series | Group | Crack spacing (mm) | |
|---|---|---|---|
| 1 | S1_05 | - | - |
| | S1_10 | - | - |
| | S1_15 | 6.8 | |
| | | 9.8 | |
| | | 7.4 | |
| | | 7.3 | Average |
| | | 9.5 | 8.2 |
| | S1_20 | 7.5 | |
| | | 9.5 | |
| | | 7.6 | |
| | | 5.8 | Average |
| | | 5.20 | 7.1 |
| 2 | S2_05 | - | |
| | S2_10 | 9.5 | |
| | | 5.9 | |
| | | 7.3 | |
| | | 10.4 | Average |
| | | 8.6 | 8.3 |
| | S2_15 | 5.8 | |
| | | 6.6 | |
| | | 5.4 | |
| | | 5.7 | Average |
| | | 4.9 | 5.7 |
| | S2_20 | 5.5 | |
| | | 5.8 | |
| | | 3.6 | |
| | | 4.2 | Average |
| | | 4.5 | 4.7 |

## 5 PREDICTION OF CRACK SPACING AND THE EXPERIMENTAL RESULTS

The average crack spacing, which generally exhibits a large scatter, is not representative of the cracking phenomenon that inevitably affects cement-based composites. For this reason, in reinforced concrete structures, not a single value but a range of possible crack spacing values has been defined by Fantilli et al.[10]. The same range can also be computed for SHCC [7], in which the values of the possible crack spacing are evaluated for a given volume fraction of long fibers (see Fig.3). However, to introduce such a range for all the hybrid composites investigated in this project, the parameter $k_B$ has to be estimated for each Series from the experimental results reported in Table 4.

### 5.1 Series 1

If $k_B = 1200$ MPa/mm is assumed for all the specimens of Series 1, most of crack spacing values are within the range bordered by the curves $l_{tr}$ - $V_f$ and 2 $l_{tr}$-$V_f$ [Eq.(1)] and depicted in Fig.6. For these cement-based composites, Eq.(3) gives $V_{f,cr} = 1.1$ % as the minimum amount of HDR in order to have a SH-SHCC. Nevertheless, when $V_f = V_{f,cr}$, only fibers longer than the adopted HDR (fiber length $L_f$ =30 mm) can generate multiple cracking and an average crack spacing value ranged by the minimum and the maximum theoretical distances ($l_{tr}$ and 2 $l_{tr}$, respectively). In general, the multiple cracking regime is possible if the half-length of the fiber is longer than the maximum crack spacing (i.e., $2\, l_{tr} < L_f/2$ ). Thus, Fig.6 suggests $V_f = 1.4\%$ as the minimum volume fraction of long steel fibers. For these reasons, the specimens S1_05 and S1_10 do not show neither strain hardening nor multiple cracking.

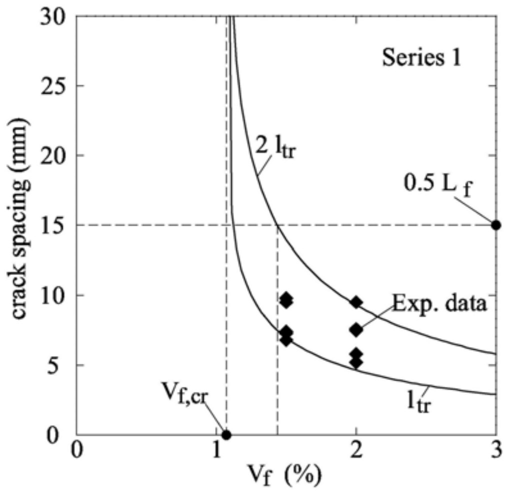


**Figure 6**: Range of possible crack spacing values in the HS-SHCC of Series 1.

### 5.2 Series 2

If $k_B = 2100$ MPa/mm is assumed for almost all the specimens of Series 2, all the measured crack spacing values are inside the range bordered by the curves $l_{tr}$-$V_f$ and 2 $l_{tr}$-$V_f$ (Fig.7). Moreover, for the composites of this Series, Eq.(3) gives $V_{f,cr} = 0.8\%$, even if, at $V_f = V_{f,cr}$, only HDR longer than 30 mm can generate an average crack spacing ranged by $l_{tr}$ and 2 $l_{tr}$. Conversely, Fig.7 seems to suggest $V_f \cong 1$ % as the minimum volume fraction of the adopted HDR (Table 2). Thus, the volume of long fibers cannot be lower than 1 %, if a SHCC has to be tailored. For this reason, only the specimens reinforced with 0.5 % of HDR do not show neither multiple cracking, nor strain hardening (see Table 4 and Fig.7).

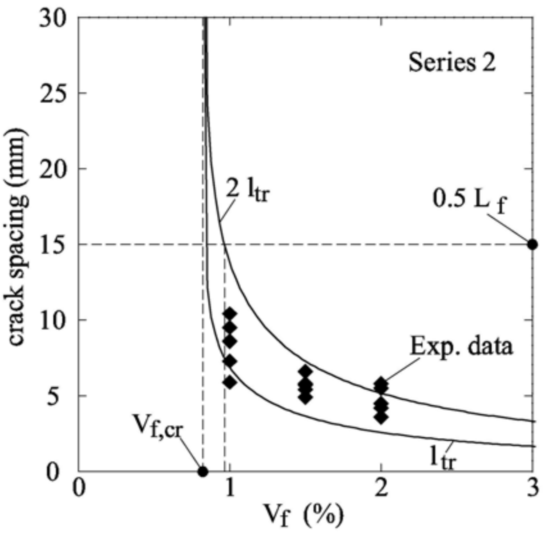


**Figure 7**: Range of possible crack spacing values in the HS-SHCC of Series 2.

## 6 CONCLUSIONS

Eqs.(1)-(3), obtained from a cohesive interface model, can be effectively used to analyse different types of very ductile composites. In the case of the High Strength SHCC investigated in the present paper, the minimum amount of long steel fibers can be effectively defined by these equations. Specifically, strain hardening and multiple cracking occur in mono-fiber composites reinforced with more than 1.5 % of HDR. Conversely, in Hybrid fiber-reinforced composites, whose matrix is already reinforced by 1% of short OL fibers, a lower volume of HDR (i.e., 1 %) is sufficient to obtain a very ductile high strength composite.

## REFERENCES


[1] Mehta, P.K. and Monteiro, P.J.M, 2006. *Concrete - Microstructure, Properties, and Materials.* McGraw-Hill.

[2] Kim, D.J., Park S. H., Ryu G. S. and Koh K. T., 2011. Comparative flexural behaviour of Hybrid Ultra High Performance Fiber Reinforced Concrete with different macro fibers. *Construction and Building Materials* **25:** 4144-4155

[3] Banthia, N. and Sappakittipakorn, M., 2007. Toughness enhancement in steel fiber reinforced concrete through fiber hybridization. *Cement and Concrete Research* **37**: 1366–1372.

[4] Stahli, P. and van Mier, J.G.M., 2007. Manufacturing, fibre anisotropy and fracture of hybrid fibre concrete. *Engineering Fracture Mechanics* **74**: 223-242.

[5] Betterman, L.R., Ouyang, C. and Shah, S.P., 1995. Fiber-matrix interaction in microfiber-reinforced mortar. *Advanced Cement Based Materials* **2**: 53-61.

[6] Kawamata, A., Mihashi, H. and Fukuyama, H., 2003. Properties of Hybrid Fiber Reinforced Cement-based Composites. *Journal of Advanced Concrete Technology*, **1**: 283-290.

[7] Fantilli, A.P., Mihashi, H. and Vallini, P. 2009. Multiple cracking and strain hardening in fiber-reinforced concrete under uniaxial tension. *Cement and Concrete Research* **39**: 1217-1229.

[8] Bazant, Z.P. and Becq-Giraudon, E., 2002. Statistical prediction of fracture parameters of concrete and implications for choice of testing standard. *Cement and Concrete Research* **32**: 529-556.

[9] Japan Society of Civil Engineers, 2008. Recommendations for Design and Construction of HPFRCC with Multiple Fine Cracks. (http://www.jsce.or.jp/committee/concrete/e/hpfrcc_JSCE.pdf).

[10] Fantilli, A.P., Ferretti, D., Iori ,I. and Vallini, P., 1998. Flexural Deformability of Reinforced Concrete Beams. *ASCE-Journal of Structural Engineering* **124**: 1041-1049.